Design and analysis of a flexure-based modular precision positioning stage with two different materials

Abstract.

Flexure-based micro-positioning stages are traditionally fabricated monolithically with only one type of material by electrical discharge machining for the purpose of high positioning accuracy. For the following purpose: design a micromanipulation stage with miniature dimension scale which driven by miniature piezoelectric actuator; the components can be replaced due to fatigue failure caused by repeated cyclic loading. This paper proposes a modular design of a flexure based 2-DOF precision stage with aluminum(T6-7075) material and Acrylonitrile Butadiene Styrene(ABS) plastic material. The piezoelectric actuator is adopted to drive the stage for the fast response and large output force. Moreover, the bridge type amplifier mechanism is adopted to compensate the limited stroke of the piezoelectric actuator.

Keywords: Flexure mechanism; Modular design; Kinematic analysis; Micro-positioning stage

1. Introduction

The 2-DOF flexure based positioning stage with ultrahigh precision has played an increasing role in high-precision manufacturing machine and high precision measurement instruments, such as atomic force microscopy(AFM)[1], nanoimprint lithography[2], precision machining and micro/nano manipulation[3]. Generally, the motion range of the micro and nano scale operation is within several hundreds of microns, the conventional joints can not satisfy the requirements due to assembling errors, hysteresis and backlash in the joints. To overcome these limitations, the monolithic flexure hinges are adopted as revolute joints to improve the motion accuracy for the advantages of no friction, no wear, no backlash and no need for lubrication[4],[5]. The flexure based mechanisms are capable of achieving highly precise positioning motion with flexure hinge which can provide a smooth and continuous motion via elastic deformation.

Piezoelectric actuators are able to obtain better performance on resolution and repeatability with closed loop control method compared with voice coil motor, shape memory alloy and electromagnetic actuators and it have been extensively used in academia and industria[6],[7]. The flexure-based positioning stage integrated with piezoelectric actuator has attracted much attention for its remarkable performances

and applications in bio-engineering and mechanical engineering field[8],[9]. However, the main disadvantage of the piezoelectric actuator is the limited output displacement, in order to compensate the output stroke of the piezoelectric actuator the amplification mechanism is adopted which maybe reduce resolution of the stage. During the literature review, the lever amplification mechanism, Scott-Russell amplification mechanism and bridge type mechanism are frequently adopted to amplify the stroke of the piezoelectric actuator. However, the aforementioned monolithic mechanism can not change their amplification mechanism for different requirements. add some figs Compared with the monolithic structure, the modular stage can use different type amplifier with amplification ratio to replace the original amplifier mechanism for different purposes. Generally, flexure-based positioning stage are mainly fabricated by aluminum alloy(T6-7075) and manufactured monolithically by electrical discharge machining method. From practical experience, some parts of the monolithic structure do not need same stiffness and also different components have different recycle life due to the fatigue failure caused by the repeated cyclic loading.

In this paper, a modular 2-DOF positioning stage fabricated with two different materials is proposed. As a result of using two different materials, the required maximum stress and force loading on the flexure hinge caused by piezoelectric decreased, so that the stage can be easily miniaturized, and high-force piezoelectric elements are not needed. The remainder of this paper is organized as follows: the Section 2 briefly introduced the design process of this decoupled mechanism; the Section 3 describes the principle of the modular design in detail; the simulation results are proposed in Section 4 to validate the performance of this design and the conclusions are made in Section 5.

2. Motivations of the research

The traditional monolithic precision positioning stages were generally fabricated by electrical discharging machining(EDM) method with aluminum alloy material. This kind of monolithic structure has the advantage of no assemble errors, however the disadvantages are time-cost manufacture process and the failure components cannot be replaced. Moreover, the stiffness along the driven direction can lead to displacement loss. As shown in Fig.1, mechanisms are subjected to the same constraint conditions and the solid type Quad.4 with 182 node was chosen element to mesh the stage. The output displacement of Fig.1a (maximum $31.81\mu m$) is larger than the Fig.1b($23.65\mu m$) which are both made by aluminum alloy material because the flexure guider's stiffness has lead to displacement loss. Fig.1c is the modular structure, the amplification mechanism is made by aluminum alloy and flexure guider is made by ABS material, the maximum output displacement is $31.62\mu m$. It means that to achieve the same output displacement the modular mechanism with different material require less driven force than monolithic structure fabricated by the aluminum alloy material. In other words, the high-output force piezoelectric actuator is not necessary and is much easier to miniaturize the dimension scale of the stage. Moreover, different flexure hinges have different recycle

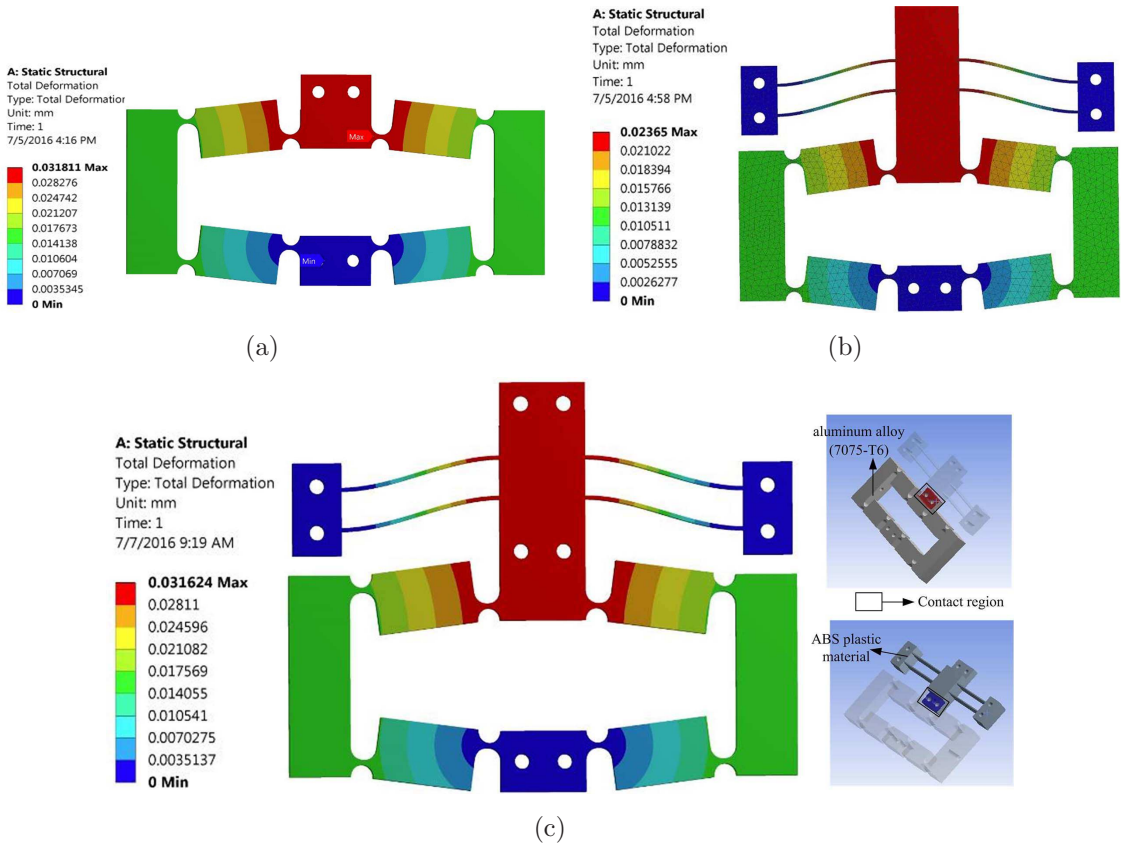

Figure 1. Output displacement comparison under 10N driven force. (a),Simulation of bridge type amplifier with maximum deformation 31.811μm; (b),Simulation of bridge type amplifier with flexure guider with maximum deformation 23.65 μm;(c),Output displacement simulation of assembled bridge amplifier and flexure guider with maximum deformation 31.624μm

life in the monolithic structure due to the repeated cyclic loading. Referring to the simulation results shown in Fig.2, the bridge type amplifier mechanism will be broken first with the 15 μm input displacement. In this scenario, the loading ratio is $R = 0$ for the reason of property of piezoelectric actuator. It means that when applying a input displacement to the monolithic stage, the bridge type amplification mechanism is more easier to broke than flexure guider mechanism. For modular structure, each parts can be replaced easily when one modular is fail to service.

each modular can be changed easily for different requirements. For example, the right circular hinge bridge type amplifier can be replaced by leaf type bridge type amplification mechanism, even it can be replaced by other type amplification mechanism, such as lever and Scott-Russell amplification mechanism.

3. The Principle of Modular Design

The basic idea underlying modular design is to organize a complex system, such as an electronic system, mechanical system and large program, as a set of distinct components

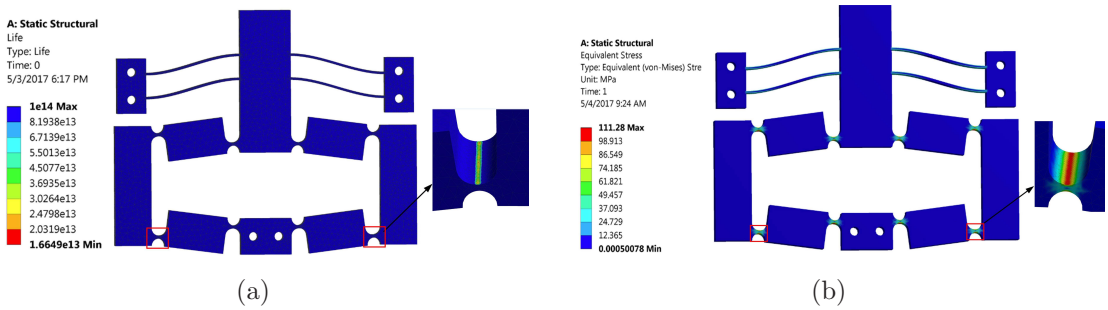

Figure 2. Fatigue and stress analysis under 15μm input displacement. (a), Life cycles simulation with minimum life cycles 1.6649e13; (b), Stress analysis with the maximum stress 111.28MPa.

that can be developed independently and then plugged together[14]. Although this seems appear a simple idea, the design principles are not only particularly relevant to parallel design but also can reduce the cost. In the micro/nano manipulation field, stages are mainly manufactured monolithically without assembling. Some advantages of this kind design can improve the positioning precision and reduce the assembling time. However, every coin has two sides, from the practical experience, the different parts of the monolithic structure undertake varies stress and deformation, it means that the different components have different recycle life due to the repeated cyclic loading. To save the cost, the modular components can be replaced when it fail to service due to fatigue failure[15].

The conventional monolithic micro manipulation stage fabricates with aluminum alloy material by electrical discharging machining method is depicted in Fig.3. This monolithic manipulation stage can be divided into four main components for their different function, amplifier mechanism: to compensate the limited stroke of the piezoelectric actuator; flexure guider mechanism: to avoid/reduce the parasitic motion perpendicular to the driven direction; parallelogram flexure: to partially decouple the motion along X/Y direction, and end-effector-to support the objects. During the literature review, some researchers divided the micromanipulation stage in more detail, beams and flexure hinges such as primitive flexures for the reason of the flexure hinge plays critical function in micromanipulation stage. However, the assembling process is time costly and will produce more errors. In order to avoid these disadvantages, this study proposes a modular 2-DOF micromanipulation stage based on each component's function.

The proposed modular 2-DOF micro-positioning stage is depicted in Fig.4, which consists of a bridge type amplification modular, flexure guider modular, parallelogram flexure modular and a mobile platform modular and the dimension scale of this designed modular stage is $157 \times 157mm$. During the actuation, the amplification mechanism will generate the parasitic motion, so a flexure guider modular is needed to avoid/reduce this kind of motion. However, the stiffness of flexure guider modular will cause the displacement loss, So flexure guider modular should be made by soft material.

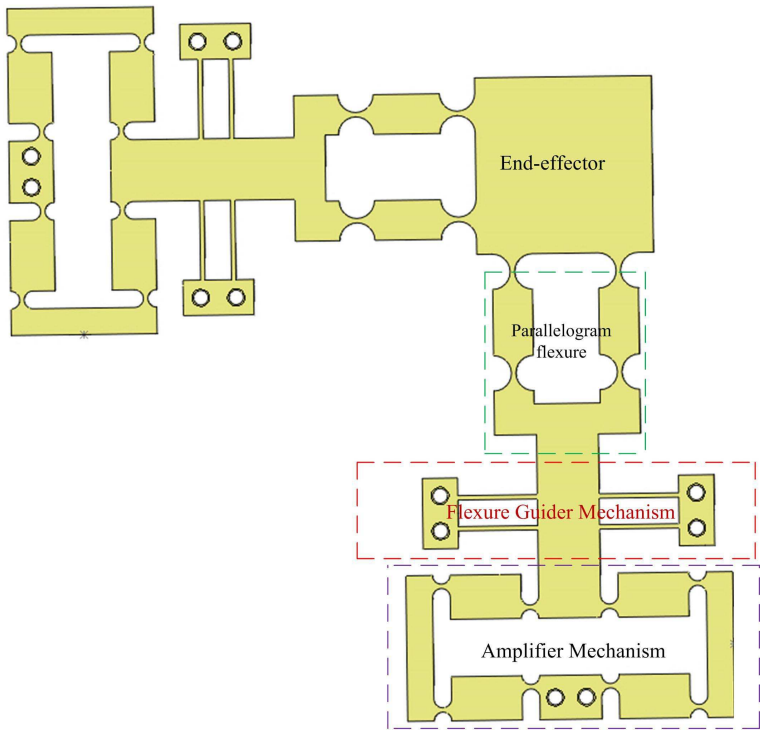

Figure 3. Traditional decoupled 2-DOF monolithic flexure-based positioning stage

The right circular hinge is adopted as revolute joint for its better rotation accuracy compared with other type of flexure hinge. The P-810.10 piezoelectric actuator with the maximum push force $50N$ and travel range $15\mu m$ made by PI, *inc* is chose to drive the manipulation stage. To compensate the stroke of the piezoelectric actuator, the bridge type amplification mechanism is adopted for its fully symmetric structure is able to reduce the thermal effect and parasitic motion. In this paper, the ABS material $(E = 1.1GPa, \sigma = 25MPa, CTE = 7.8e^{-5}mm/^{\circ}C)$is adopted to fabricate flexure guider mechanism, parallelogram flexure and end-effector; the aluminum alloy material T6-7075 $(E = 71.7GPa, \sigma = 505MPa, CTE = 2.36e^{-5}mm/^{\circ}C)$is adopted to fabricate the bridge type amplifier mechanism. The modular stage should working constant temperature environment because the adopted material has the different coefficient of thermal expansion (CTE) coefficient.

4. Manipulation Stage Analysis

In order to simplify the analysis process, the schematic diagram of the designed flexure based parallel mechanism is shown in Fig.5. The reference frame xoy is attached on the center of GF with the distance of $2d$, G, F denotes the end-point of each flexure guider mechanism respectively, at the initial status the reference point P is on the Y axis. The input force/displacement through bridge type amplifier and flexure guider mechanism to drive the mobile platform. As depicts in Fig.5, the spring denotes the total stiffness of bridge type amplifier and flexure guider mechanism along the driven direction, through

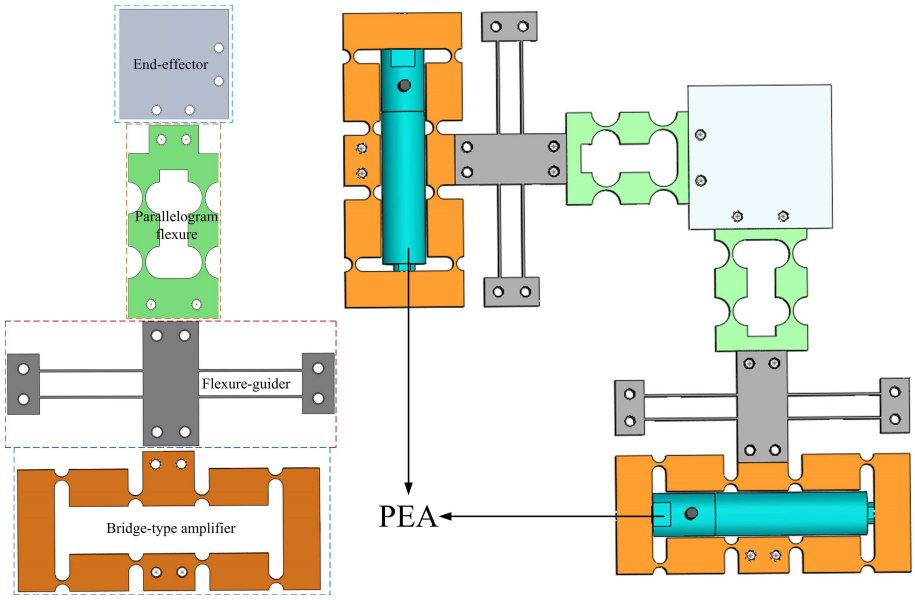

Figure 4. The modular flexure-based positioning stage

Table 1. Architectural parameters of the stage

parameter	value(mm)	parameter	value(mm)	parameter	value(mm)	parameter	value(mm)
t	0.8	h	8.8	d	36.77	c	20
r	4	w	8	b	34	a	15.6

the simulation the value of the $K_{b+f} = 316.36N/mm$. The pseudo rigid body (PRB) method is adopted to model and calculate the stiffness of right circular hinge. Each flexure hinge can be replaced by a revolute joint and torsional spring, K denotes the rotation stiffness of the flexure hinge. The parameters of the designed compliant parallel manipulation are shown in Tab.1

And the K can be calculated by the following equation[16]:

$$K = \frac{2Ewt^{2.5}}{9\pi r^{0.5}} \tag{1}$$

Here, E represents the Young's Modulus of the material, and other parameters of the flexure hinge are presented in Tab.1

4.1. Bridge Type Mechanism Analysis

Bridge type amplification mechanisms are usually adopted to amplify the stroke of piezoelectric actuators because fully symmetric structure can reduce thermal effect and parasitic motion. As shown in Fig.6, which is the quarter of the bridge type amplifier, when the input voltage is applied, the piezoelectric actuators produce an input stroke and to propel the external load to move along the perpendicular direction. As shown in Fig.6 (a), when the input stroke X is applied, the bridge type amplifier will generate the output displacement Y due to the rotational angle α of the link arm. Fig.6 (b)

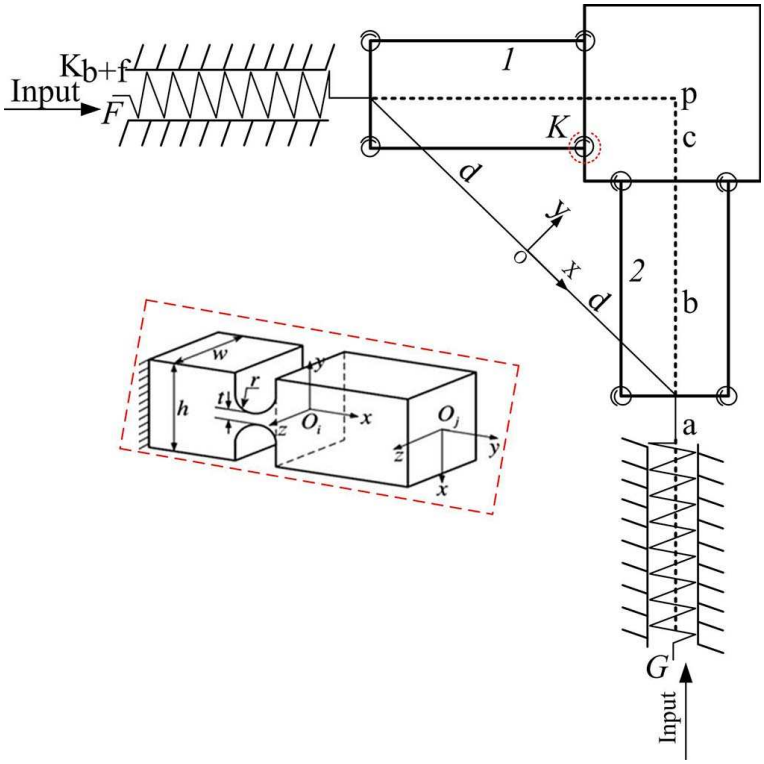

Figure 5. Schematic description of the 2-DOF flexure based parallel manipulator

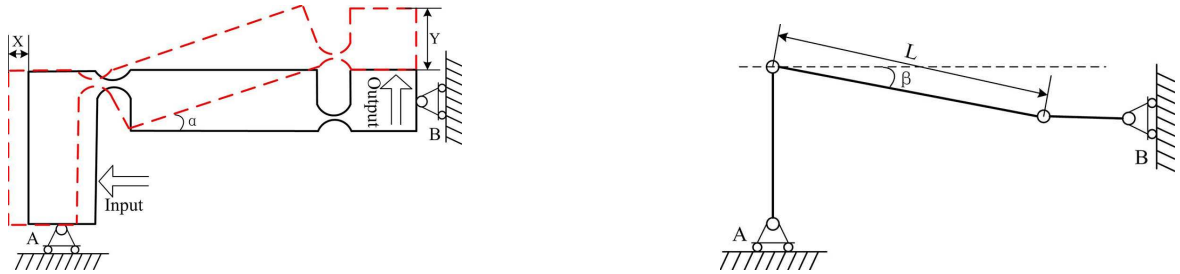

(a) (b)

Figure 6. Quarter model of bridge type amplifier mechanism.(a),Schematic deformation model. (b),Kinematic model

depicts kinematic model of quarter bridge type amplifier. Here β denotes initial incline angle of the link arm; L denotes the total length of the link arm and flexure hinges. Therefore, the input displacement and output displacement can be written as a function of geometric relations:

$$X = L(\cos(\beta - \alpha) - \cos\beta) \tag{2}$$

$$Y = L(\sin\beta - \sin(\beta - \alpha)) \tag{3}$$

So the amplification ratio of the bridge type amplifier can be derived as:

$$R_{amp} = \frac{Y}{X} = \frac{\sin\beta - \sin(\beta - \alpha)}{\cos(\beta - \alpha) - \cos\beta} = \cot\beta \tag{4}$$

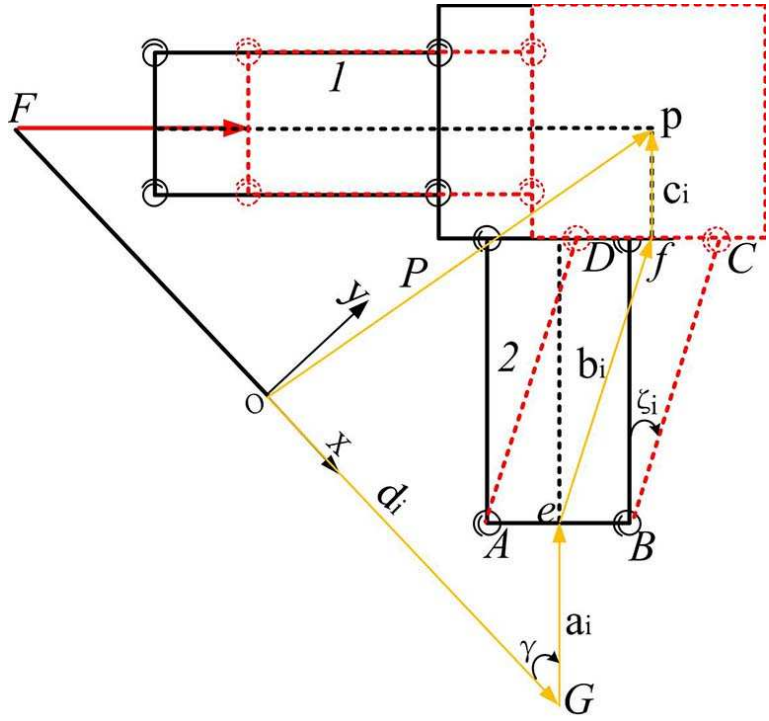

Figure 7. Traditional decoupled 2-DOF monolithic flexure-based positioning stage

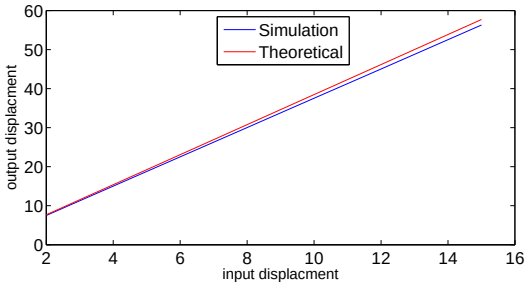

Figure 8. Theoretical results vs. simulation results of the amplification ratio.

Here, we assume that the rotation angle $\alpha \to 0$.

Based on the architectural parameters of the designed mechanism, the value of the $\beta = 14.57deg$, the theoretical amplification ratio is 3.8473. To validate the theoretical analysis, the simulation has been conducted via Workbench software, the maximum output displacement of the flexure guider is $56.297\mu m$ when the piezoelectric actuator achieves full input. Referring to the Fig.8 in which the amplification ratio is 3.753, the error is about 2.4%.

4.2. Kinematic Analysis

As shown in Fig.7, the mobile platform is connected with two identical parallelograms, the points e, f denote the center point of the AB and CD, respectively. The vectors $\overrightarrow{ef}$ and $\overrightarrow{fp}$ with the fixed length b and c have the same direction. Let define $\mathbf{r} = [r_1, r_2]^T$ be

the input vector applied on the parallelogram joint variables, where the $r_i = R_{amp}q_i$, q_i denotes the output stroke of the piezoelectric actuator, $(i = 1, 2)$. The position of the mobile platform in the reference frame xoy is denoted by the vector $\mathbf{p} = [x, y]^T$.

4.2.1. inverse kinematic analysis The inverse kinematic is to solve the exact values of the actuators with given the position of the mobile platform. Referring to the yellow line as shown in Fig.7, a vector-loop equation can be written as follows:

$$\overrightarrow{P} = d\overrightarrow{d_i} + r\overrightarrow{a_i} + b\overrightarrow{b_i} + c\overrightarrow{c_i} \tag{5}$$

Where $\overrightarrow{d_i}$ is the unit vector of $\overrightarrow{oG}$, $\overrightarrow{a_i}$ is the unit vector of $\overrightarrow{Ge}$, $\overrightarrow{b_i}$ is the unit vector of $\overrightarrow{ef}$ and $\overrightarrow{c_i}$ is the unit vector of $\overrightarrow{fp}$, here $\overrightarrow{a_i} = \overrightarrow{c_i} = (-\widetilde{c}\gamma, \widetilde{s}\gamma)$. $\widetilde{c}$ stands for cos, $\widetilde{s}$ stands for sin.

Here, we define $\overrightarrow{m_i} = \overrightarrow{p} - d\overrightarrow{d_i} - c\overrightarrow{a_i}$, so the following equation can be derived:

$$\overrightarrow{m_i} - r_i\overrightarrow{a_i} = b\overrightarrow{b_i} \tag{6}$$

So the q_i can be solved by the above equation. Due to the configuration of this parallel mechanism, only negative square roots are chosen for actuated values and they can be written as:

$$q_1 = \frac{1}{R_{amp}}(x + d)\widetilde{c}\gamma + y\widetilde{s}\gamma - c - \sqrt{b^2 - [(x + d)\widetilde{s}\gamma - y\widetilde{c}\gamma]^2} \tag{7}$$

$$q_2 = \frac{1}{R_{amp}}(d - x)\widetilde{c}\gamma + y\widetilde{s}\gamma - c - \sqrt{b^2 - [(d - x)\widetilde{s}\gamma - y\widetilde{c}\gamma]^2} \tag{8}$$

Thus, the output stroke of the piezoelectric actuators can be solved by the above (7) and (8) equations.

4.2.2. Forward kinematic analysis The forward kinematics is to solve the position of the mobile platform given a set of input values of the actuators. To solve the mobile platform position x, y, define $\overrightarrow{n_i} = d\overrightarrow{d_i} + (r + c)\overrightarrow{a_i}$. Based on the equation (5), the following equation can be derived:

$$\overrightarrow{p} - \overrightarrow{n_i} = b\overrightarrow{b_i} \tag{9}$$

So the following equation can be obtained by dot-multiplying the equation (9) with itself:

$$x^2 + y^2 - 2n_ix - 2n_iy + 2n_i^2 = b^2 \tag{10}$$

Also the equation (10) can be expanded as the following two equations:

$$[x + d - (r_1 + c)\widetilde{c}\gamma]^2 + [y - (r_1 + c)\widetilde{s}\gamma]^2 = b^2 \tag{11}$$

$$[x - d + (r_2 + c)\widetilde{c}\gamma]^2 + [y - (r_2 + c)\widetilde{s}\gamma]^2 = b^2 \tag{12}$$

Where $r_i = R_{amp}q_i$, referring to the equation (11) and (12), it means that the solutions of the forward kinematic are located at the intersection of the two circles which the radius is b and the center of the two circles are $(-d + (r_1 + c)\widetilde{c}\gamma, (r_1 + c)\widetilde{s}\gamma)$ and $(d - (r_2 + c)\widetilde{c}\gamma, (r_2 + c)\widetilde{s}\gamma$, respectively.

4.3. Static Analysis

The relationship between applying force and displacement of the mobile platform can be derived through the static analysis. The PRB method can simplify the analytical process of flexure based compliant mechanism. As shown in Fig.7, the black line denotes the initial position of the micro manipulation stage and red line denotes the position after applying the actuation force. With applying the driven force $F_i(i = 1, 2)$, the parallelogram will have a rotational angle $\delta_i(i = 1, 2)$ and mobile platform will have a displacement $d_i(i = 1, 2)$ along the actuation direction. The force-deflection relationship can be derived as follows:

$$F_1 = \frac{4K(\delta_2)}{(r_2 + bc\delta_2 + c)} + K_{b+f}r_1 \qquad F_2 = \frac{4K(\delta_1)}{(r_1 + bc\delta_1 + c)} + K_{b+f}r_2 \tag{13}$$

Where $\delta_i, (i = 1, 2)$ denotes the rotational angle of the parallelogram $ABCD$, K is the stiffness of the flexure hinge.

The dynamic performance of the stage is decided by the natural frequency of mechanism, which has an influence on the sensitiveness to the environmental vibrations. However, these characteristics are mainly derived from experiment, which will be conducted in our future work. The modal simulation of the designed stage is presented in Section 5.

4.4. Workspace Analysis

The workspace of the micromanipulator can be defined as the space that can be reached by the reference point P attached on the mobile platform. Parallel mechanism have a relatively small workspace, compared with serial mechanism. One of the purposes the proposed modular stage is to get a large workspace with piezoelectric actuators. Thus, the workspace is an important index to evaluate the performance of the micromanipulator.

4.4.1. Constraint condition 1: limited input stroke As mentioned above, the adopted piezoelectric electric actuator has limited stroke. Here, the maximum displacement of the adopted actuator is Q, so the following inequation can be derived:

$$0 \leq q_i \leq Q \tag{14}$$

Where $i = 1, 2$. As aforementioned, the equation (11) and (12) representing the two circles and the intersection area of the circles subjected to the piezoelectric actuator motion range limits can be derived. Thus, the workspace $W_{(x,y)}$ subject to stroke of piezoelectric actuator can be derived by following equations:

$$W_{(x,y)} = S_{(11)} \bigcap S_{(12)} \tag{15}$$

4.4.2. Constraint condition 2: limited rotation scope of flexure hinge The maximum rotational scope of the flexure hinge depends on the elastic modulus of the material. Let the δ_i^m, $(i = 1, 2)$ be the maximum rotational angle of the link BC relative to its

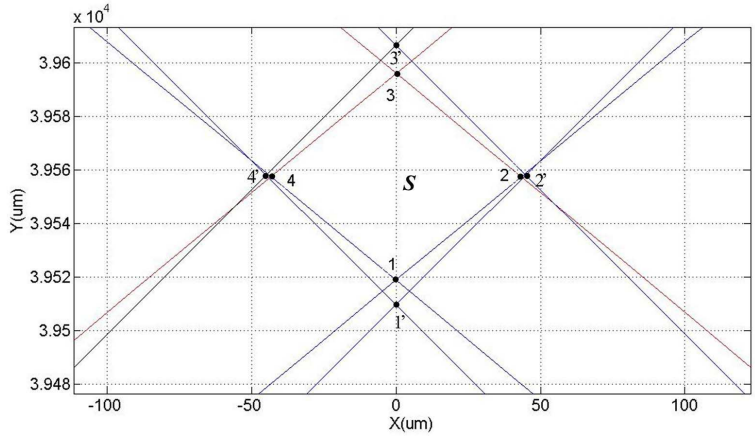

Figure 9. Reachable workspace of the designed modular stage: X[-46.5μm, +46.5μm]; Y[39.50mm, 39.593mm].

the initial position angle δ_i^0. When the maximum angle δ_i^m arises, the maximum stress σ_{max} occurs at the outermost point of the flexure hinge with minimum thickness t, let the yield strength be σ_y, thus:

$$\sigma_{max} = \frac{K_i \delta_i^m (t/2)}{I} = \frac{6 K_i \delta_i^m}{w t^3} = \sigma_y \tag{16}$$

Where $I = wt^3/12$, and K_i is the stiffness of the parallelogram.
The workspace of the manipulator subjected to the rotational scope of the flexure hinge can be written as $|\delta_i| \leq \delta_i^m$, so $-\delta_i^m \leq \delta_i - \delta_i^0 \leq \delta_i^m$. Then the following inequation can be derived:

$$\tan(\delta_i^0 - \delta_i^m) \leq \tan(\delta_i) \leq \tan(\delta_i^0 + \delta_i^m) \tag{17}$$

So the constraint inequation can be expressed as:

$$\tan(\delta_1^0 - \delta_i^m) \leq \frac{y - (r_1 + c)\widetilde{s}\gamma}{x + d - (r_1 + c)\widetilde{c}\gamma} \leq \tan(\delta_1^0 + \delta_1^m) \tag{18}$$

$$\tan(\delta_2^0 - \delta_i^m) \leq \frac{y - (r_2 + c)\widetilde{s}\gamma}{x - d + (r_2 + c)\widetilde{c}\gamma} \leq \tan(\delta_2^0 + \delta_2^m) \tag{19}$$

Thus, the workspace of the manipulation stage can be calculated by the equations (11),(12),(18) and (19).

Based on the aforementioned kinematic analysis, constraint conditions and architecture parameters of the mechanism, the workspace of the mechanism can be derived. As shown in Fig.9, the area S_{1234} denotes the workspace subjected to the limited stroke of the piezoelectric actuators; the area $S_{1'2'3'4'}$ denotes the workspace subjected to the rotational limits of the flexure hinges. Obviously, the workspace of the stage is the intersection of these two areas ($S_{1234} \bigcap S_{1'2'3'4'}$). Referring to the Fig.8, the reachable workspace area of this mechanism is S_{1234}, which mainly determined by the output stroke of the piezoelectric actuators.

Table 2. The comparison results simulated by finite element analysis.

Items / Material	Output displacement x(μm)	Output displacement y(μm)	Coupling ratio (%)	First natural frequency (Hz)	Maximum stress (MPa)
A.A	1.24	11.78	10.52	384.05	152.56
ABS	78.25	723.57	10.81	81.37	4.78
A.A-ABS	4.57	95.71	4.77	92.42	4.57

5. Simulation Results and Discussions

In this paper, a 2-DOF modular positioning stage fabricated with two different materials: aluminum and ABS is proposed. Here, the amplifier mechanism and end-effector are made by 7075-T6, the flexure guider mechanism is made by ABS material. To validate the performance of the proposed stage, simulations have been conducted in Workbench software environment. The FEM analysis results of the precision positioning stages which fabricated by the aluminum alloy (A.A)(7075-T6), ABS and aluminum alloy-ABS (A.A-ABS) materials are shown in Tab.2, respectively. The simulation results of end-effector about displacement, coupling ratio, natural frequency and maximum stress are shown in Tab.2 and the simulation results are depicted in Fig.10 which under the case of $30N$ driven force. Referring to the Tab.2, the stage made by A.A-ABS material has relative large displacement under the equal driven force compared with that of other stages. In the other words, to get the equal output displacement, the miniature piezoelectric actuator can be adopted to drive the designed modular stage. The output displacement simulated by the FEA validates the computational workspace, although it has approximately 2.83% error. Moreover, compared with the monolithic structure with the same architectural parameters, the modular structure has less coupling ratio. Although the total symmetric structure can reduce the coupling ratio, it will improve the stiffness of the structure caused by the displacement loss and increase the cost.

6. Conclusion

A 2-DOF modular compliant parallel mechanism utilizing two different materials is presented in this paper. Based on the function of each component, the monolithic structures are divided into four parts: amplification mechanism, flexure guider mechanism, parallelogram flexure and end-effector. So the manipulation stage can be assembled by these modules for different purposes. Meanwhile, the proposed stage is analyzed by the developed PRB model, the kinematics and force deflection relationship are derived. Taking the stroke of the piezoelectric and rotational scope constraints into consideration, the computational workspace of this modular manipulator is about $93 \times 93\mu m$ which will satisfy the design goals. In addition, the FEA is conducted by Workbench software to compare the characteristics of the monolithic structure and modular structure and validates that the modular structure has good linearity. The

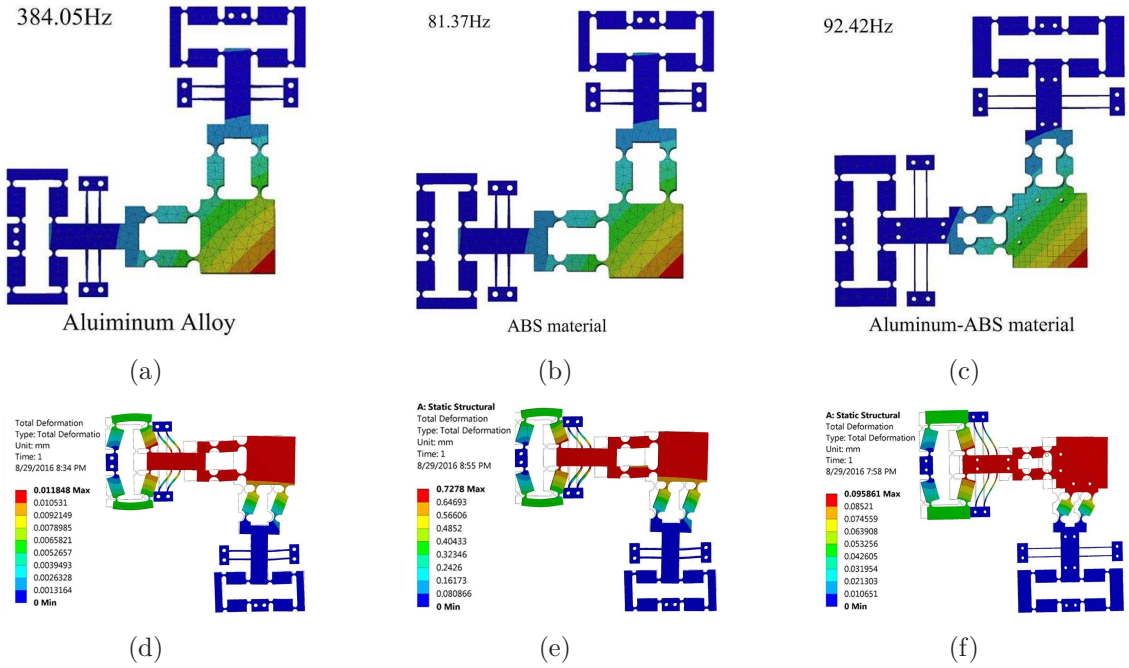

Figure 10. Dynamic and static characteristic performance of each stage. (a),the first modal of monolithic A.A stage; (b),the first modal of monolithic ABS material stage; (c),the first modal of modular A.A-ABS material stage; (d), the static deformation along X axis of the A.A stage; (e), the static deformation along X axis of the ABS stage; (f), the static deformation along the X axis of the A.A-ABS stage.

dynamic characteristics analysis, error analysis and positioning accuracy of the modular stage will be conducted in our future work. Moreover, developing some modules which can be used to assemble a planar and spatial stage for different purposes is our another goal.

References

[1] Schittera, G., Thurner, P. J. and Hansma, P.K. (2008), "Design and input-shaping control of a novel scanner for high-speed atomic force microscopy", *Mechatronics*, Vol.18, pp. 282-288.

[2] Teo, T.J., Yang, G.L. and Chen, I.M. (2014), "A large deflection and high payload flexure-based parallel manipulator for UV nanoimprint lithography: Part I. Modeling and analyses", *Precision Engineering*, Vol.38, pp.861-871.

[3] Li, Y.M. and Xu, Q.S.(2012), "Design and robust repetitive control of a new parallel-kinematic xy piezostage for micro/nanomanipulation", *IEEE/ASME Transactions on Mechatronics*, Vol.17, No.6, pp.1120-1132.

[4] Ding, B.X. and Li, Y.M.(2014), "Design and analysis of a decoupled xy micro compliant parallel manipulator", *IEEE International Conference on Robotics and Biomimetics*, pp.1898-1903.

[5] Goldfarb,M. and Speich,J.E.(1999), "A well-behaved revolute flexure joint for compliant mechanism design", *Transactions of the ASME, Journal of Mechanical Design*, Vol.121, pp.424-429.

[6] Ang,W.T., Khosla,P.K. and Riviere, C. N.(2007), "Feedforward controller with inverse rate-dependent model for piezoelectric actuators in trajectory-tracking applications",*IEEE/ASME Transactions on Mechatronics*, Vol.12, No.2, pp.134-142.

[7] Ding,B.X., Li,Y.M., Xiao, X. and Tang, Y.R.(2016), "Optimized PID tracking control for piezoelectric actuators based on the Bouc-Wen Model", *IEEE International Conference on Robotics and Biomimetics*, pp.1576-1581.

[8] Qi, K.Q., Xiang, Y., Fang, C., Zhang, Y. and Yu, C.S.(2015), "Analysis of the displacement amplification ratio of bridge-type mechanism", *Mechanism and Machine Theory*, Vol.87, pp.45-56.

[9] Hao,G.B., and Hand,R.B.(2016), "Design and static testing of a compact distributed-compliance gripper based on flexure motion", *Archives of Civil and Mechanical Engineering*, Vol.16,No.4,pp.708-716.

[10] Yong,Y.K., Aphale,S.S. and Moheimani,S.O.R.(2009), "Design, identification, and control of a flexure-based xy stage for fast nanoscale positioning", *IEEE Transactions on Nanotechnology*, Vol.8, No.1,pp.46-54.

[11] Tian,Y.L., Shirinzadeh, B., Zhang, D. W. and Alici, G. (2009), "Development and dynamic modelling of a flexure-based Scott-Russell mechanism for nano-manipulation", *Mechanical Systems and Signal Processing*, Vol.23, pp.957-978.

[12] Li, Y.M. and Xu, Q.S.(2012), "A novel piezoactuated XY stage with parallel,decoupled, and stacked flexure structure for micro-/nanopositioning", *IEEE Transactions on Industrial Electronics*, Vol.58, No.8, pp.3601-3615.

[13] Jung,H.J. and Kim,J.H.(2014), "Fabrication of piezo-driven micropositioning stage using 3D printer, *Journal of the Korean Society for Precision Engineering*, Vol.31, No.3, pp.277-283.

[14] Farritor,S., Dubowsky,S.,Rutman,N. and Cole,J.(1996), "A systems-level modular design approach to field robotics", *IEEE International Conference on Robotics and Automation*,pp.2890-2895.

[15] Yu,J.J., Xu,P., Sun, M.L., Zhao,S.S., Bi,S.S. and Zong,G.H. (2009), "A new large-stroke compliant joint & micro/nano positioner design based on compliant building blocks", *ASME/IFToMM International Conference on Reconfigurable Mechanisms and Robots*. 409-416

[16] Meng,Q.L., Li, Y.M. and Xu,J. (2013)"New empirical stiffness equations for corner-filleted flexure hinges", *Mechanical Sciences*, Vol.4, pp.345-356.